



# The impact of gradual increase in moisture on the collapse of Brazilian clayey sand soil

Renan Felipe Braga Zanin<sup>1</sup> · Amanda Maehara Kondo<sup>1</sup> · Flávia Gonçalves Pissinati Pelaquim<sup>2</sup> · Alana Dias de Oliveira<sup>1</sup> · Sandro Lemos Machado<sup>3</sup> · Avacir Casanova Andrello<sup>4</sup> · Raquel Souza Teixeira<sup>1</sup>

Received: 23 November 2022 / Accepted: 13 December 2023 / Published online: 30 December 2023  
© Springer-Verlag GmbH Germany, part of Springer Nature 2023

## Abstract

Soil collapse is a critical factor contributing to various pathologies in civil construction, necessitating the use of suction-controlled techniques, often unavailable in smaller cities in developing countries. This study investigated the collapsible behavior of clayey sand from Tuneiras do Oeste, Paraná, Brazil, using conventional one-dimensional tests with varied initial moisture contents and pre-soaking stresses. Tests maintained constant specimen moisture, soaked samples at pre-defined stress values (S tests), and observed collapse behavior under gradual wetting (GIM tests). Supplementary mercury intrusion porosimetry (MIP) analyses determined the collapse's influence on pore size distribution. Collapse indexes were computed, and the Pereira and Fredlund (J Geotech Geoenviron Eng 126:907–916, 2000) model was applied to predict collapsible behavior for GIM tests data, showing strong agreement with experimental results ( $R^2 > 0.98$ ). Additionally, two prediction models developed from different test data also exhibited a high degree of correlation ( $R^2 = 0.97$  and  $0.95$  for S and GIM tests, respectively). It was observed that pre-soaking moisture, i.e., the pre-soaking matric suction, played a crucial role in wetting-induced soil collapse, while pre-soaking stress had a secondary effect. The infiltration rate during soaking impacted the observed collapse, with higher rates resulting in greater collapse magnitudes. Regarding soil structure, collapse led to significant alterations only in the macropores, causing a notable reduction in their diameters. Ultimately, the experimental protocol developed in this study yielded valid results for modeling collapsible soils, even in the absence of sophisticated suction-controlled equipment.

**Keywords** Collapsible behavior · Matric suction · Porosimetry · SWCC · Collapse-predictive model · Tropical soil

## Introduction

Collapse strains pose significant damage potential, primarily affecting small buildings with shallow foundations situated on the superficial layers of evolved tropical soils. In tropical regions, the frequency of collapsible soils is

associated with regional pedogenic processes, and the collapse potential is magnified by the common occurrence of moisture levels far from saturation throughout most of the year (Houston et al. 2001; Rao and Revanasiddappa 2002; Pereira et al. 2005; Zeng and Meng 2006; Zorlu and Kasapoglu 2009).

✉ Renan Felipe Braga Zanin  
renanzanin@uel.br

Amanda Maehara Kondo  
amanda.kondo@icloud.com

Flávia Gonçalves Pissinati Pelaquim  
fgoncalves@professores.utfrpr.edu.br

Alana Dias de Oliveira  
oliveira.alana@uel.br

Sandro Lemos Machado  
smachado@ufba.br

Avacir Casanova Andrello  
acandrello@uel.br

Raquel Souza Teixeira  
raquel@uel.br

<sup>1</sup> Department of Civil Construction, State University of Londrina, Londrina, Paraná, Brazil

<sup>2</sup> Academic Department of Civil Construction, Federal Technological University of Paraná, Pato Branco, Paraná, Brazil

<sup>3</sup> Department of Materials Science and Technology, Federal University of Bahia, Salvador, Bahia, Brazil

<sup>4</sup> Department of Physics, State University of Londrina, Londrina, Paraná, Brazil

Li and Vanapalli (2018) and Alassal et al. (2023) have indicated that the magnitude of collapse is inversely related to the initial soil moisture: the lower the initial moisture, the higher the matric suction value and, consequently, the more significant the energy released upon soil saturation, causing more considerable compressible volumetric strains. Regarding pre-soaking stress, the relationship with collapse is direct: for a given initial moisture content, an increase in imposed vertical stress results in greater collapse strains. However, this increase typically continues only until a certain maximum stress value, beyond which the collapse strains start to decrease (Gutierrez et al. 2008; Ferreira and Fucalé 2014; Borges et al. 2016).

Moreover, as noted by Ferreira (1995), collapse strains resulting from the breakdown of solid particle connections appear to be associated with the soil's water penetration rate (i.e., the infiltration rate). It is crucial to note that the infiltration rates in laboratory tests are typically higher than those in the field. The abrupt soaking process to which soil samples are subjected in one-dimensional tests for collapse evaluation is rarely, if ever, encountered in the field, except in case of anthropogenic events, such as the failure of functional water pipelines.

Structurally, collapse can be defined as the outcome of macropore compression due to soaking and/or loading, without notable changes in micropore volume (Jiang et al. 2014; Yu et al. 2022). Li et al. (2018) have posited that collapse initially impacts the macropores and if the process progresses the micropores may be affected. Other researchers have also suggested that, throughout the compression process, macropores may be converted into micropores (Yu et al. 2016; Wang et al. 2020). Investigating the influence of the collapse strains on the soil structure and pore size distribution can provide insights into the mechanisms underlying the collapse of a specific soil formation.

Although it is well-established that suction-controlled tests offer advantages over traditional ones, as they allow for the imposition and control of suction, thereby providing greater flexibility in test execution, there are considerable resource distribution challenges in developing countries with vast territorial expanses, such as Brazil, China, and Russia. Most available resources are concentrated in coastal cities, and as unsaturated soils are known to be extremely demanding in terms of time and resources, small- to medium-sized cities located far from the coast often lack access to the necessary equipment to conduct a comprehensive experimental program, which typically involves suction-controlled tests. The limited suction-controlled equipment available is usually found at universities in the larger cities and state capitals. Consequently, in such situations, traditional

one-dimensional compression tests with constant moisture content are more accessible and practical, as they are simpler and yield reliable results (Jennings and Knight 1975; Silva Filho et al. 2010; Vilar and Rodrigues 2011).

Therefore, this research aimed to assess the feasibility of an experimental simplified protocol, utilizing conventional and readily available techniques and equipment, to yield coherent results regarding soil collapsible behavior. Several undisturbed soil specimens from the city of Tuneiras do Oeste, Paraná, Brazil, were subjected to a one-dimensional test procedure, employing different pre-soaking stresses and moisture contents. The Soil–Water Retention Curve (SWRC) of the specimens facilitated the correlation between moisture content and suction, aiding in understanding the influence of suction on collapse. Additionally, the occurrence of collapse under the gradual wetting process was evaluated. The obtained results were meticulously analyzed with a focus on the observed compressive volumetric strains and comprehensive assessment of the impact of these strains on the soil's pore size distribution.

## Material and methods

### Material

The material under investigation is a residual soil, characteristic of the Northwest region of Paraná, in the Southeast region of Brazil. Undisturbed samples were collected near the city of Tuneiras do Oeste (23°48'50.3" S, 52°59'58.8" W), at an elevation of 410 m above sea level, and from approximately 2 m below the surface.

Table 1 summarizes the principal geotechnical properties of the soil. It is evident that the soil exhibits medium plasticity and is classified as clayey sand (SC) by the Unified Soil Classification System (USCS), considering the fractions obtained with the use of deflocculant (ASTM 2017). The particle size distribution points to the existence of natural micro-aggregation in the clay fraction, which is disintegrated when the soil is treated with the deflocculant, as noted by Oliveira et al. (2022).

Figure 1 illustrated the obtained SWRC (main drying branch). Matric suction was ascertained/enforced using two distinct methods: pressure plate (for suctions below 1000 kPa) and filter paper. The SWRC experimental points were fitted using Eq. 1, proposed by Gitirana and Fredlund (2004), for bimodal pore size distributions, substituting the saturation degree with volumetric moisture content ( $\theta$ ) in the original equation.

$$\theta = \frac{\theta_1 - \theta_2}{1 + \left( \frac{\psi}{\sqrt{\psi_{b1} * \psi_{res1}}} \right)^{d_1}} + \frac{\theta_2 - \theta_3}{1 + \left( \frac{\psi}{\sqrt{\psi_{res1} * \psi_{b2}}} \right)^{d_2}} + \frac{\theta_3 - \theta_4}{1 + \left( \frac{\psi}{\sqrt{\psi_{b2} * \psi_{res2}}} \right)^{d_3}} + \theta_4 \quad (1)$$

**Table 1** Characteristics of the soil

Soil characteristic			Value	Standard
Liquid limit— $w_L$ (%)			20	NBR 6459 (ABNT 2016b)
Plastic limit— $w_P$ (%)			13	NBR 7180 (ABNT 2016c)
Plasticity index— $I_P$ (%)			7	
Particle density— $\rho_s$ (g/cm <sup>3</sup> )			2.89	NBR 6458 (ABNT 2016a)
Particle size distribution	With deflocculant	Clay (%)	21	NBR 7181 (ABNT 2016d)
		Silt (%)	4.7	
		Sand (%)	74.3	
	Without Deflocculant	Clay (%)	2	
		Silt (%)	23.7	
		Sand (%)	74.3	

**Fig. 1** SWRC for Tuneiras do Oeste soil

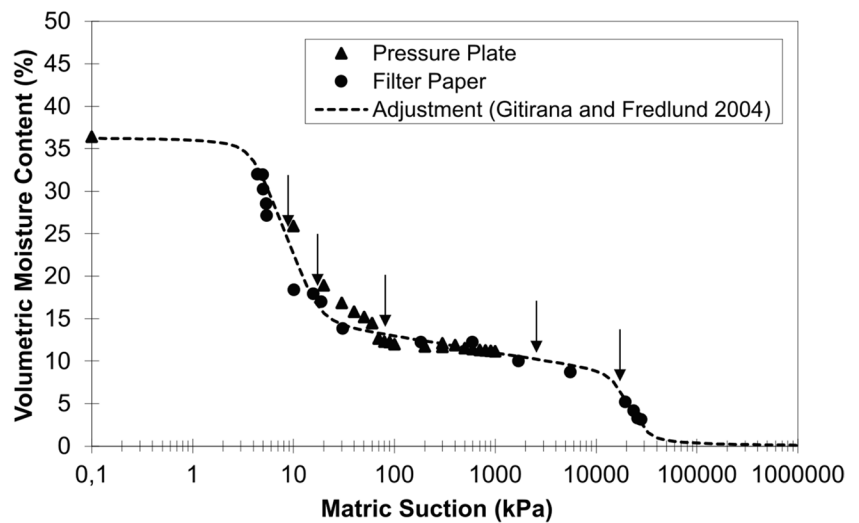


**Table 2** Parameters of the SWRC fitting equation by Gitirana and Fredlund (2004), considering the volumetric ( $\theta$ ) moisture contents

Parameter	$\theta_1$ (%)	$\theta_2$ (%)	$\theta_3$ (%)	$\theta_4$ (%)	$\psi_{b1}$ (kPa)	$\psi_{b2}$ (kPa)	$\psi_{res1}$ (kPa)	$\psi_{res2}$ (kPa)	$d_1$	$d_2$	$d_3$
Value	36.39	13.86	9.10	0.05	4	18,000	17	27,000	3.992	2.309	23.558

where  $\theta_1$  to  $\theta_4$  are volumetric moisture contents that denote the beginning and end of the individual hyperbolas;  $\psi$  is the soil matric suction;  $\psi_{b1}$  and  $\psi_{b2}$  are the first and second air-entry values, respectively;  $\psi_{res1}$  and  $\psi_{res2}$  are the residual soil matric suctions for each desaturation path; and  $d_1$ ,  $d_2$  and  $d_3$  are the weight factors. Table 2 presents the obtained fitting parameters.

**Methods**

Undisturbed specimens, carved out with nominal dimensions of 8 cm in diameter and 3.2 cm high, were used in all one-dimensional compression. The tests were conducted using a conventional one-dimensional compression apparatus, adhering to the procedures outlined in ASTM (2021) and ASTM (2020), unless otherwise specified in this paper.

**Table 3** Values chosen for gravimetric ( $w$ ) and volumetric ( $\theta$ ) moisture contents and respective estimated matric suctions ( $\psi$ )

$w$ (%)	$\theta$ (%)	$\psi_{estimated}$ (kPa)
17.0	25.0	8.5
11.0	16.1	18
9.0	13.2	80
7.0	10.3	2500
5.0	7.3	16,000

The initial moisture contents of the specimens under test were determined to evaluate the influence of suction on soil behavior using two different experimental procedures. These procedures were selected based on the curve presented in Fig. 1. Five initial moisture content values were chosen to cover the following SWRC regions (indicated by arrows in

Fig. 1), as detailed in Table 3: after the first air-entry value; the onset of the intermediate level (transition between macro and micropores); two values in the midst of the transition phase, before the second air-entry value; and one residual moisture content, following the second air-entry value.

The adopted experimental procedures were the standard one-dimensional test performed on saturated samples, one-dimensional compression with one-step soil saturation, and one-dimensional compression with a gradual increase in soil moisture.

### Tests performed with one-step saturation (S)

These tests were conducted by loading the specimen at a presumably constant moisture content until the stress of interest was reached. The specimens were then saturated by soaking, and the loading process resumed after stabilizing the volumetric strains (very low variation of the second decimal place in the sample's height) (ASTM 2021). Three different soaking stresses were adopted (50, 100, and 200 kPa) for each non-saturated initial moisture content (see Table 3), resulting in fifteen experiments.

### Tests performed with gradual increase in moisture

Gradual increase in moisture (GIM tests) simulated the soil response to a process of gradual suction reduction. Samples were gradually wetted by dripping at the vertical stresses of 50, 100, and 200 kPa, with initial moisture contents of 5, 7, and 9%, totaling nine experiments. Depending on the samples' initial moisture content, moistening occurred in steps to values of 7, 9, 11, and 17% and then saturation (final moisture content of about 25%). These moisture contents were chosen from the SWRC (as shown in Table 3) and enabled a wide range of matric suction to be analyzed during wetting.

### Collapse-predictive models

The GIM test results were fitted by applying the model proposed by Pereira and Fredlund (2000). This model assumes that the soil collapse process comprises three phases: pre-collapse, where minor volume variations occur under high suction values; collapse, where significant deformations occur under intermediate suction values; and post-collapse, where minimal or zero deformations occur under low suction values. The results of the S tests were not adjusted for this model due to the soaking method used, in only one step, making it challenging to analyze the three phases of the collapse. The authors propose Eq. 2 to simulate the soil volumetric behavior in the three phases mentioned above.

$$e = e_i + \frac{e_f - e_i}{\left[1 + \left(\frac{\psi}{c}\right)^b\right]^a} \quad (2)$$

where  $e$  stands for the void ratio,  $e_i$  and  $e_f$  are the initial and final void ratios, respectively,  $\psi$  is the soil matric suction,  $c$  is the suction value at the inflection point (midpoint on the collapse phase line),  $b$  is the collapse phase line slope, and  $a$  is symmetry parameter that makes the logistic function asymmetric. Several researchers (e.g., Ercoli et al. 2015; Al-Obaidi and Schanz 2022; Giomi and Francisca 2022) have proven over time the application of what was proposed by Pereira and Fredlund's (2000) model, indicating in fact the existence of the three phases of the collapse.

In addition, using the LAB Fit® curve fitting software (Silva and Silva 2022) and nonlinear regression analyses, two new models were developed to characterize the behavior of the soil studied in this paper. The models were developed to best fit the data found from the software's library of equations.

### Mercury intrusion porosimetry tests

Mercury intrusion porosimetry (MIP) tests were conducted on six specimens to assess the impact of the collapse strains on the soil's pore size distribution. The selected samples had initial moisture contents of 5% and 11% and were saturated at the same vertical stresses as previously described. These results were then juxtaposed with the findings from the MIP test conducted on a natural, undisturbed soil sample.

Post the one-dimensional compression tests, the samples underwent a drying process in an oven, following which specimens, approximately 1 cm in nominal dimensions, were extracted for the MIP tests (ASTM 2018). For this test, the specimen was positioned in a penetrometer, the volume of which was already known and consisted of a glass beaker and a metal-coated rod. Once the mass of the entire setup was measured, the penetrometer was affixed to the equipment and subsequently sealed.

The penetrometer was initially filled with mercury without exerting any pressure, thereby preventing the metal from infiltrating the soil's voids. This step enabled the determination of specimen volume by calculating the difference between the penetrometer and the mercury volumes. Finally, pressures were incrementally applied, ranging from approximately 0.7 to 414,000 kPa, until the mercury permeated all soil voids.

## Results and discussions

Table 4 presents the initial physical properties of the specimens utilized in all the S and GIM tests, along with certain statistical parameters associated with the soil properties. It is evident that the coefficient of variation (COV) values,

which is the ratio of the standard error and the mean, of the soil properties are within the expected range. This shows a tolerable variability between samples, as corroborated by Phoon and Kulhawy (1999), Duncan (2000), Baecher and Christian (2003), and Branco et al. (2014). Moreover, the obtained COV values align with the typical ranges observed for residual soils (Gutierrez et al. 2008).

### Tests performed with one-step saturation (S)

To mitigate the impact of the initial void ratio on the compression curves, the experimental data were normalized using the initial void ratio of each specimen, resulting in curves originating

from the same point (Jennings and Knight 1957). Figure 2 illustrates the normalized curves derived from the S tests.

As anticipated, specimens with lower initial moisture content exhibited less compression before soaking and tended to exhibit higher collapse strains upon wetting (Vilar and Davies 2001; Benatti and Miguel 2013). Conversely, the specimens with higher initial moisture content exhibited lower estimated values of matric suction, facilitating the formation of weaker inter-particle bonds, and thereby inducing instability in the soil microstructure. Consequently, increased levels of compression were observed for stresses applied prior to soaking (Basma and Tuncer 1992, Das and Thyagaraj 2016, Phanikumar et al. 2016, Zamani and Badv 2019 and Alassal et al. 2023).

**Table 4** Physical indexes of the specimens of S and GIM tests

$\sigma_{soak}$ (kPa)	Test denomination	Physical Indexes							
		w <sup>a</sup> (%)	$\rho^b$ (g/cm <sup>3</sup> )	$\rho_d^c$ (g/cm <sup>3</sup> )	$\theta^d$ (%)	e <sup>e</sup>	n <sup>f</sup> (%)	S <sub>r</sub> <sup>g</sup> (%)	
50	S-50-17	18.01	1.73	1.46	26.36	0.97	49.36	53.41	
	S-50-11	12.06	1.64	1.46	17.66	0.97	49.31	35.81	
	S-50-09	9.39	1.59	1.46	13.68	0.99	49.62	27.56	
	S-50-07	7.78	1.67	1.55	12.05	0.87	46.39	25.98	
	S-50-05	4.95	1.51	1.44	7.12	1.01	50.23	14.17	
	GIM-50-09	9.08	1.46	1.34	12.13	1.16	53.75	22.57	
	GIM-50-07	6.85	1.40	1.31	8.98	1.20	54.64	16.44	
	GIM-50-05	5.00	1.49	1.42	7.09	1.04	50.92	13.92	
100	S-100-17	18.06	1.73	1.47	26.48	0.97	49.25	53.77	
	S-100-11	12.32	1.69	1.50	18.53	0.92	47.93	38.67	
	S-100-09	10.19	1.64	1.48	15.13	0.95	48.62	31.11	
	S-100-07	8.20	1.64	1.52	12.42	0.91	47.57	26.11	
	S-100-05	6.38	1.53	1.44	9.17	1.01	50.27	18.25	
	GIM-100-09	8.95	1.52	1.40	12.51	1.07	51.65	24.22	
	GIM-100-07	6.96	1.58	1.48	10.30	0.95	48.79	21.11	
	GIM-100-05	5.31	1.51	1.43	7.59	1.02	50.50	15.03	
200	S-200-17	17.59	1.77	1.51	26.55	0.92	47.78	55.55	
	S-200-11	12.33	1.65	1.47	18.11	0.97	49.16	36.84	
	S-200-09	9.95	1.62	1.47	14.67	0.96	48.99	29.95	
	S-200-07	7.57	1.56	1.45	10.96	1.00	49.90	21.96	
	S-200-05	5.29	1.41	1.34	7.10	1.15	53.59	13.24	
	GIM-200-09	8.98	1.55	1.42	12.74	1.04	50.90	25.03	
	GIM-200-07	6.95	1.47	1.38	9.57	1.10	52.34	18.28	
	GIM-200-05	5.23	1.54	1.46	7.65	0.98	49.45	15.46	
Mean		–	1.58	1.44	–	1.00	50.04	–	
Standard deviation			0.10	0.06		0.08	2.02		
COV (%)			6.33	4.17		8.00	4.04		

<sup>a</sup>Gravimetric moisture content

<sup>b</sup>Density of the soil

<sup>c</sup>Dry density of the soil

<sup>d</sup>Volumetric moisture content

<sup>e</sup>Void ratio

<sup>f</sup>Porosity

<sup>g</sup>Saturation degree

**Fig. 2** Normalized curves of S tests for soaking stresses of (a) 50 kPa, (b) 100 kPa, and (c) 200 kPa

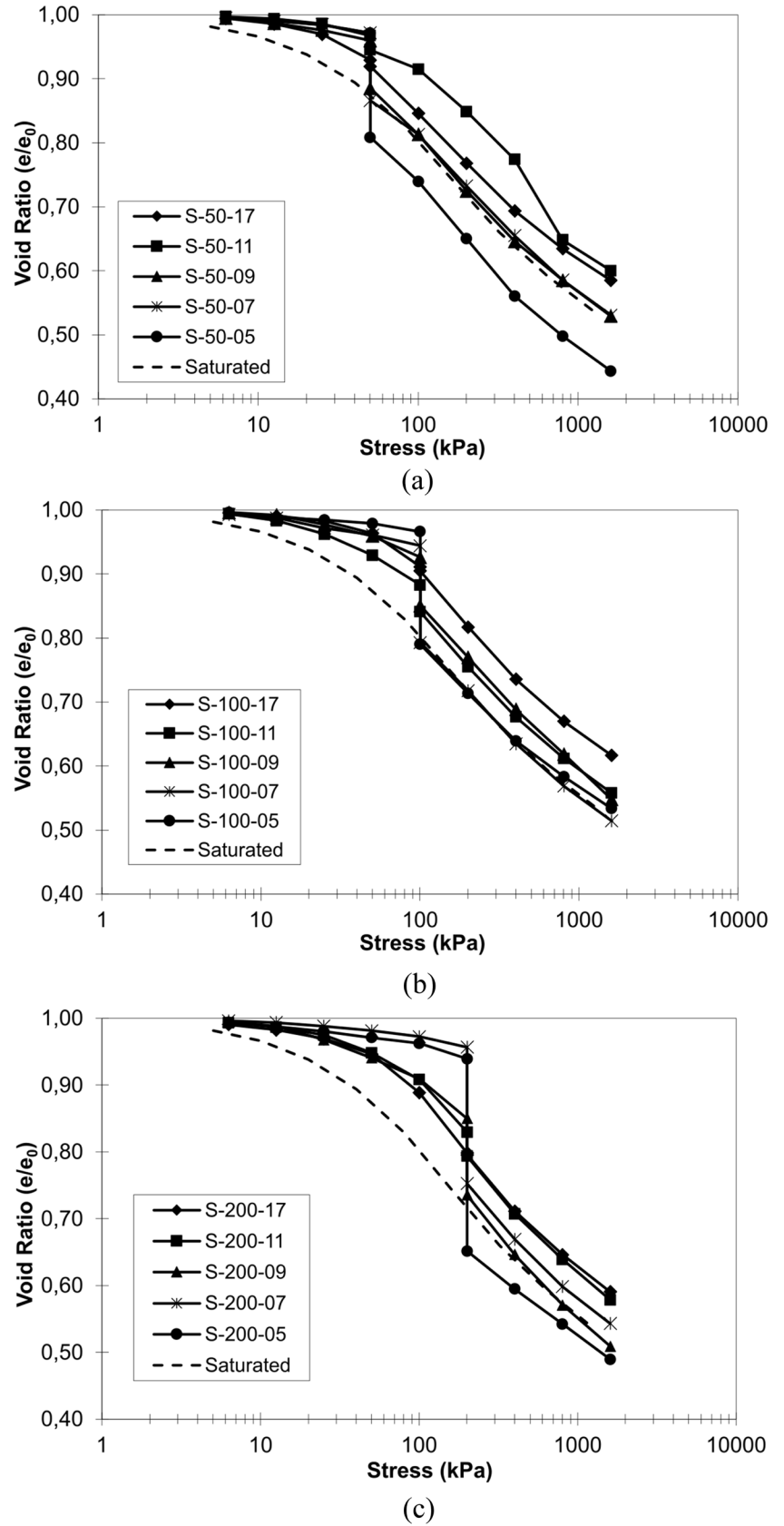
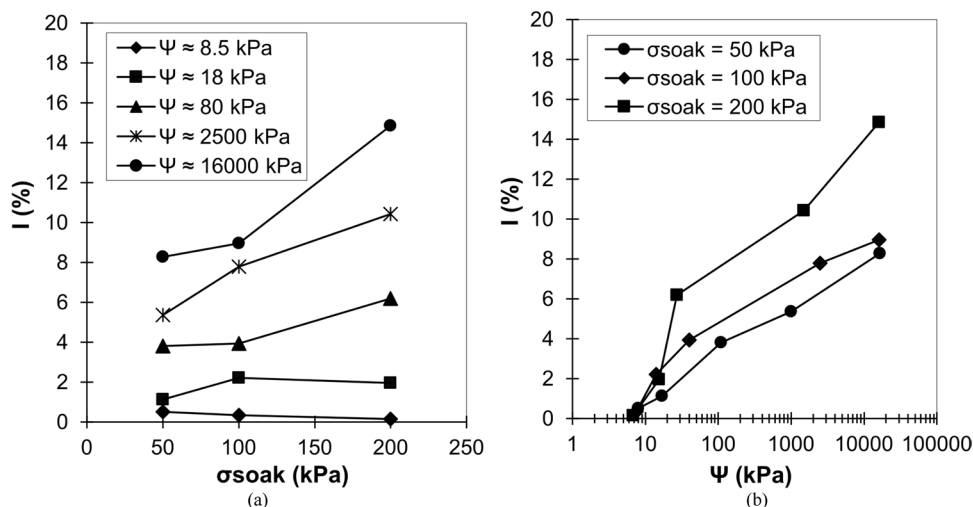


**Fig. 3** Collapse index (*I*) versus (a) soaking stress ( $\sigma_{soak}$ ) and (b) estimated matric suction ( $\Psi$ )



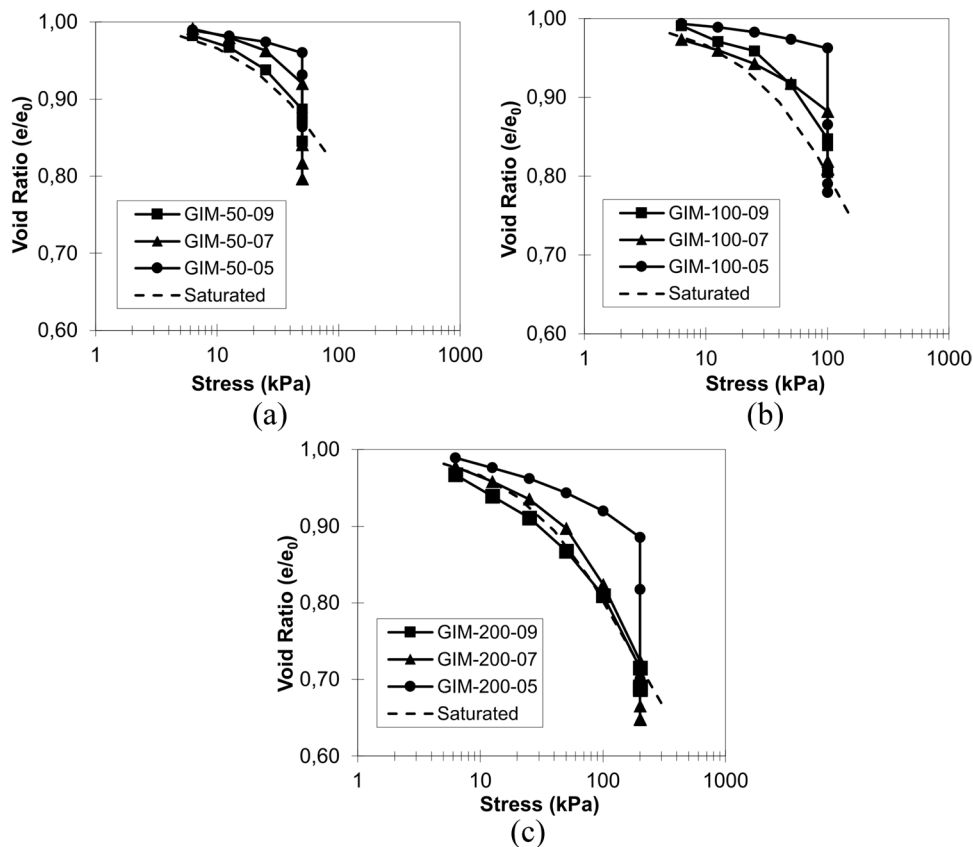
Collapse indexes were computed utilizing the data presented in Fig. 2, adhering to the criteria delineated by Jennings and Knight (1975). These findings are illustrated in Fig. 3. Equation 3 presents the collapse index proposed by the authors.

$$I = \frac{\Delta e}{1 + e_i} \tag{3}$$

where *I* denotes the collapse index,  $\Delta e$  represents the void ratio variation attributed to soaking, and  $e_i$ , the void ratio prior to soaking.

Analyzing the Fig. 3a, it is evident that the soil’s response to different soaking stresses for the same suction value is not uniform. At lower suctions (8.5 kPa and 18 kPa), collapse strains typically remain below 2.5%, with no discernible trend of increase with vertical stress. This outcome was expected, as the soil suction in this scenario was inadequate to significantly enhance its stiffness, resulting in compressions under loading like to those observed in saturated samples. For suctions of 80 kPa and above, both soil compression and the collapse index exhibited an

**Fig. 4** Normalized curves of the GIM tests under stresses of (a) 50 kPa, (b) 100 kPa, and (c) 200 kPa



uptrend with the exerted vertical stress. These observations align with the findings of Pereira and Fredlund (2000), Phanikumar et al. (2016), Li et al. (2019), and Alassal et al. (2023), where the magnitude of strains induced by collapse escalated with the applied stress.

Moreover, even at the lowest soaking stress, the collapse index for samples with suctions of 80 kPa and above was substantial. This phenomenon can be attributed to the diminution of sizeable natural voids between sand particles, caused by disintegration of clay micro-aggregates during soaking, as noted by Alassal et al. (2023).

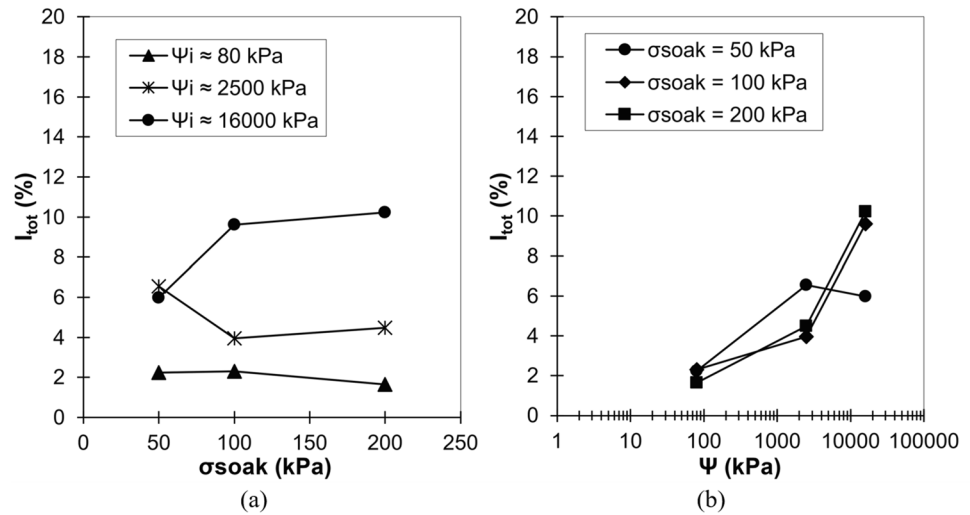
As shown in Fig. 3b, soil compression evidently increases with the pre-soaking suction, which is consistent with the data delineated by Vilar and Davies (2001), Vilar and Rodrigues (2011), Phanikumar et al. (2016), and Li and Vanapalli (2018). These studies indicate that samples with higher initial matric suction levels liberate more energy upon saturation, thereby inducing greater strains due to collapse. This also reaffirms the assertion made by Benatti et al. (2011) that collapse is a conditional state rather than an intrinsic soil property, as it hinges on the moisture content (i.e., suction) at which it is encountered — a condition that is subject to alteration.

**Table 5** Accumulated collapse indexes and problem classification for each increase of moisture

$\sigma_{\text{soak}}$ (kPa)	Test denomination	Increase of moisture (%)	$\Psi_{\text{estimated}}$ (kPa)	$I_{\text{accum}}$ (%)	Classification (Jennings & Knight 1975)	
50	GIM-50-09	09 → 11	80 → 18	0.75	No Problem	
		11 → 17	18 → 8.5	2.20	Moderate	
		17 → 25	8.5 → ≈ 0	2.24	Moderate	
	GIM-50-07	07 → 09	2500 → 80	4.13	Moderate	
		09 → 11	80 → 18	5.45	Problematic	
		11 → 17	18 → 8.5	6.53	Problematic	
	GIM-50-05	17 → 25	8.5 → ≈ 0	6.56	Problematic	
		05 → 07	16,000 → 2500	1.47	Moderate	
		07 → 09	2500 → 80	4.01	Moderate	
	100	GIM-100-09	09 → 11	80 → 18	5.00	Moderate
			11 → 17	18 → 8.5	5.95	Problematic
			17 → 25	8.5 → ≈ 0	5.98	Problematic
		GIM-100-07	07 → 09	2500 → 80	3.37	Moderate
			09 → 11	80 → 18	3.86	Moderate
			11 → 17	18 → 8.5	3.93	Moderate
200	GIM-100-05	17 → 25	8.5 → ≈ 0	3.95	Moderate	
		05 → 07	16,000 → 2500	4.95	Moderate	
		07 → 09	2500 → 80	8.20	Problematic	
	GIM-200-09	09 → 11	80 → 18	8.99	Problematic	
		11 → 17	18 → 8.5	9.58	Problematic	
		17 → 25	8.5 → ≈ 0	9.61	Problematic	
200	GIM-200-07	07 → 09	2500 → 80	1.45	Moderate	
		09 → 11	80 → 18	1.60	Moderate	
		11 → 17	18 → 8.5	1.65	Moderate	
	GIM-200-05	17 → 25	8.5 → ≈ 0	1.65	Moderate	
		05 → 07	16,000 → 2500	3.41	Moderate	
		07 → 09	2500 → 80	3.41	Moderate	
	GIM-200-05	09 → 11	80 → 18	4.43	Moderate	
		11 → 17	18 → 8.5	4.47	Moderate	
		17 → 25	8.5 → ≈ 0	4.49	Moderate	
GIM-200-05	05 → 07	16,000 → 2500	3.60	Moderate		
	07 → 09	2500 → 80	10.04	Serious		
	09 → 11	80 → 18	10.13	Serious		
GIM-200-05	11 → 17	18 → 8.5	10.19	Serious		
	17 → 25	8.5 → ≈ 0	10.22	Serious		



**Fig. 5** Total collapse index ( $I_{tot}$ ) versus (a) soaking stress ( $\sigma_{soak}$ ) and (b) estimated matric suction ( $\psi$ )



**Tests performed with a gradual increase in moisture**

Figure 4 shows the normalized compression curves derived from GIM tests, while Table 5 enumerates the accumulated collapse strains ( $I_{accum}$ ) induced by the incremental wetting process, categorized as per the criteria established by Jennings and Knight (1975).

An analysis of Table 5 reveals that a significant portion of the collapse predominantly occurs when soil suction decreases to 80 kPa ( $w \approx 9\%$  and  $Sr \approx 24\%$ ), especially in instances with elevated applied vertical stress values. Consistently, specimens with an initial moisture content of 9% exhibited total collapse strains of less than 2.5%.

The potential for significant collapse strains in the field, even without reaching saturation, suggests a soil structure with a high propensity for collapse. Conversely, soil saturation during precipitation events is influenced by the soil’s saturated hydraulic conductivity ( $k_{sat}$ ) and the hydraulic conductivity function, both of which are affected by the

SWRC. The balance between rainfall intensity and the soil hydraulic conductivity determines the soil suction at steady-state or the peak moisture content during the infiltration, thereby governing the magnitude of field collapse. This, in turn, is also affected by soil suction during infiltration (Van Genuchten 1980; Fredlund et al. 1994; Öberg and Sällfors 1997; Machado and Zuquette 2004).

Taking into account the accumulative compression under progressive wetting and the collapse severity classification by Jennings and Knight (1975), all specimens with an initial moisture of 5% could yield collapse strains categorized as severe or problematic (collapse indices exceeding 5%). Specimens with 7% initial moisture exhibited collapse strains exceeding 5% for 50 kPa of overburden stress and values between 3 and 5% under other loading conditions.

The data in Fig. 5 aligns with that in Fig. 3. However, the correlation between collapse and vertical stress is less pronounced. This is likely due to the compression experienced by the specimen prior to saturation, which tends to increase with

**Fig. 6** Comparison between the collapse indexes (I) of GIM and S tests under soaking stress of 50 kPa, 100 kPa, and 200 kPa

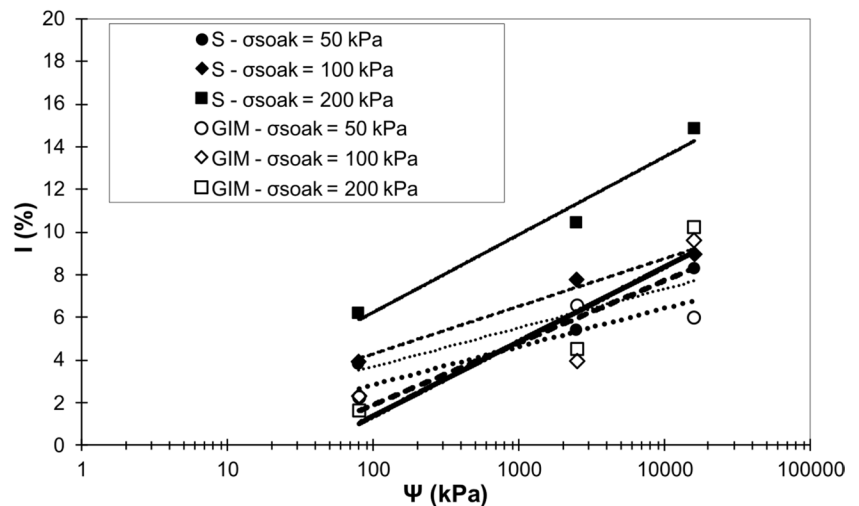


**Fig. 7** Application of the Pereira and Fredlund (2000) model to the soil under stresses of (a) 50, (b) 100, and (c) 200 kPa

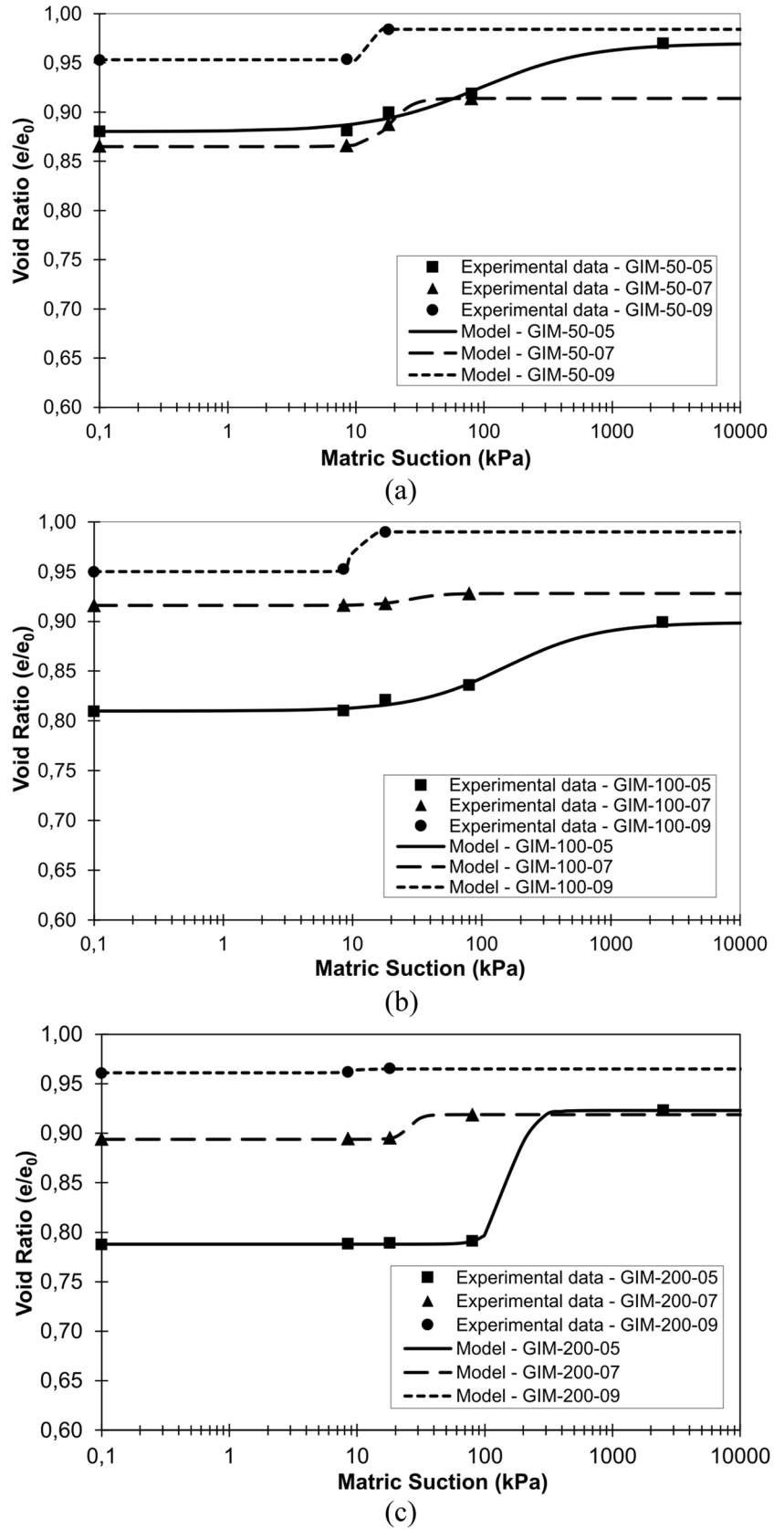


**Table 6** Parameters of the model by Pereira and Fredlund (2000) for GIM tests

$\sigma_{soak}$ (kPa)	Test denomination	Parameter					$R^2$
		$e_i$	$e_f$	$c$ (kPa)	$b$	$a$	
50	GIM-50-09	0.984	0.953	12.501	32.291	1.000	1.000
	GIM-50-07	0.914	0.865	18.770	4.891	1.000	1.000
	GIM-50-05	0.970	0.880	94.819	1.038	1.000	0.984
100	GIM-100-09	0.990	0.950	10.083	17.240	1.000	1.000
	GIM-100-07	0.928	0.916	27.737	3.555	1.000	0.992
	GIM-100-05	0.899	0.810	154.368	1.219	1.000	0.992
200	GIM-200-09	0.965	0.961	9.211	13.668	1.000	1.000
	GIM-200-07	0.919	0.894	25.645	8.975	1.000	0.998
	GIM-200-05	0.923	0.788	161.288	5.397	1.000	1.000

higher stress levels, offsetting the impact of suction on the specimen’s initial stiffness (Pereira and Fredlund 2000; Phanikumar et al. 2016; Li et al. 2019). Regarding the influence of pre-soaking suction, the results are consistent, except for the notably high collapse exhibited by specimen GIM-50-07, attributable to its relatively high initial void ratio ( $e_i = 1.20$ ).

Figure 6 contrasts the final collapse indexes derived from GIM tests with those from S tests. Predominantly, the S tests induced greater compressions rendering them more suitable for assessing potential collapse in practical scenarios; rapid wetting processes typically yield increased collapse compression. On the other hand, GIM tests are more apt for replicating the field collapse process, assuming accurate evaluation of the infiltration process.

**Collapse-predictive models**

Figure 7 demonstrates the efficacy of the model proposed by Pereira and Fredlund (2000) in simulating the results from GIM tests. Notably, there is a strong congruence between the predicted and experimental results. The three phases of collapse were distinctly delineated for majority of the conditions analyzed, with the parameters of Eq. 2 and the coefficient of determination,  $R^2$  (which quantifies the proportion of the original variance explained by the model) detailed in Table 6.

While the model from Pereira and Fredlund (2000), along with other models in the literature, involve an analysis with a single independent variable (either suction or stress), this paper proposes the creation of two models capable of predicting the soil’s collapsible behavior with two independent variables, thereby enabling a 3D analysis.

Utilizing the LAB Fit® curve fitting software and designating the soaking stress and matric suction as independent variables, the curves shown in Fig. 8 a and b were generated for both tests (S and GIM tests, respectively). The curves in Fig. 8 are characterized by Eqs. 4 and 5, respectively, with  $R^2$  values of 0.97 and 0.95.

$$I = 0.12 * (\sigma_{soak}^{0.46}) * [\ln(\Psi - 7.30)] \tag{4}$$

$$I = 2.06 * \{ \sigma_{soak}^{[(0.07 * (\ln \Psi)) - 0.38]} \} \tag{5}$$

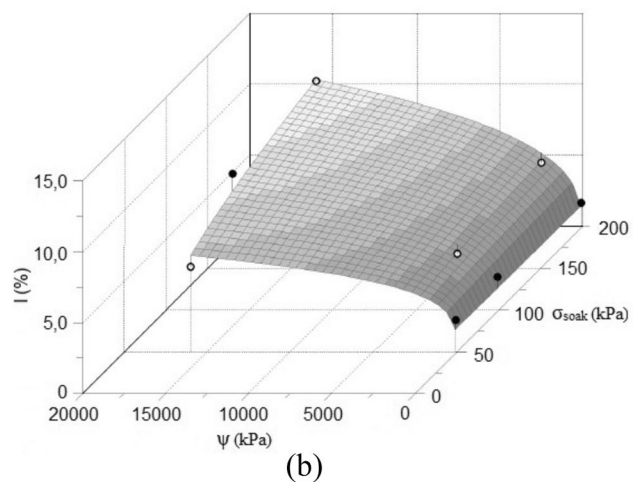
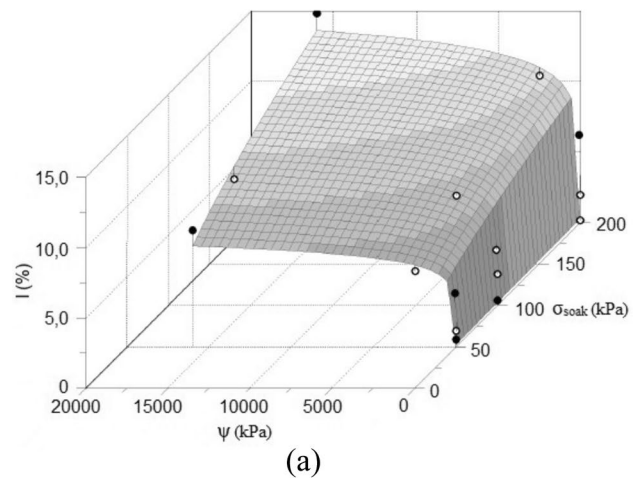


**Fig. 8** Collapse-predictive models for (a) S tests and (b) GIM tests

where  $I$  denotes the collapse index, in percentage,  $\sigma_{soak}$  represents the soaking stress, in kPa, and  $\psi$  signifies the matric suction, in kPa. Consequently, it is evident that both Eq. 4 and Eq. 5 provide a robust qualitative assessment of collapse for the investigated soil, considering the boundary conditions of the acquired data: undisturbed samples of Clayey Sand soil—SC, with natural micro-aggregation, bimodal pore distribution and  $\psi \geq 8.5$  kPa, in addition to the distinct conditions of the two separate tests for each equation.

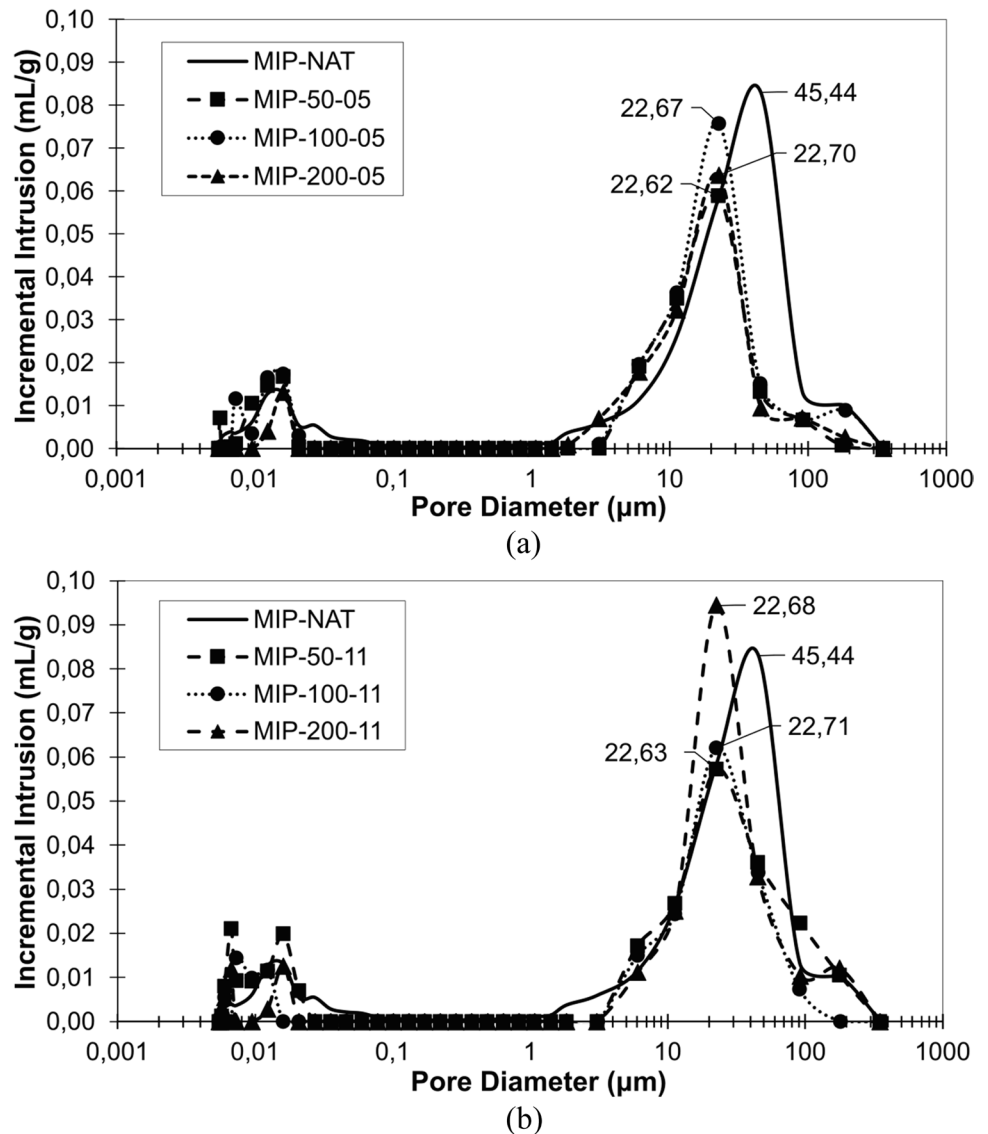
### Mercury intrusion porosimetry tests

Figure 9 illustrates the histograms of pore size frequency derived from the mercury intrusion porosimetry (MIP) tests, which were designated with the soaking stress and initial moisture content. The MIP-NAT test represents the histogram of pore size frequency for the natural soil, devoid of

any loading. It is observed that all tests feature two principal pore size groups, separated by approximately two orders of magnitude: the macropores, encompassing the range between 2 and 300  $\mu\text{m}$ , and the micropores, varying between 0.006 and 0.1  $\mu\text{m}$ , signifying a bimodal pore size distribution, consistent with the SWRC illustrated in Fig. 1.

Owing to the collapse compressions, the intervals corresponding to macropores were shifted towards the left, exhibiting a significant reduction in diameter compared to the natural soil. Evaluating the impact of initial moisture content, i.e., the initial matric suction, it is observed that the collapse induced by soaking predominantly influenced the pore volume, rather than its diameter, resulting in almost identical values at the peaks of the histograms (between 22.62 and 22.71  $\mu\text{m}$ ). Hence, samples with lower initial moisture content, or higher initial matric suction, underwent a larger reduction in the volume of macropores, particularly noticeable for samples

**Fig. 9** Histograms of pore size frequencies for initial moisture content of (a) 5% and (b) 11%



subjected to a tension of 200 kPa. This suggests that the diminution of macropores is chiefly accountable for the alteration in soil structure, leading to a modification in hydraulic behavior and water retention capacity (Yu et al. 2022).

Specifically, under uniform vertical pressures of 50, 100, and 200 kPa, the prevailing macro and micropores diameters diminished from 22.62, 22.67, and 22.70  $\mu\text{m}$  (Fig. 9a) to 22.63, 22.71, and 22.68  $\mu\text{m}$  (Fig. 9b), respectively. Conversely, the primary micropore group and its peak intensity exhibited minimal alteration post-loading and wetting. This implies that the propensity of undisturbed Clayey Sands to undergo collapse is predominantly contingent upon the reduction in size and quantity of macropores following loading and wetting, as proposed by Shao et al. (2018). The MIP data in Fig. 9 indicate that the macropores in moister samples undergo only marginal compression upon soaking. This can be attributed to the low initial matric suction values of these samples, culminating in a “meta-stable” microstructure susceptible to additional collapse during soakings (Ge et al. 2019).

The micropore volume exhibited only marginal variation, as documented by Jiang et al. (2014) and Yu et al. (2022). Romero et al. (2011) and Yu et al. (2021) contend that the micropore volume may diminish during soaking due to the swelling and dispersion of clay particles. However, this volume tends to be recovered due to some drying processes, such as that the samples went through for the MIP tests. Consequently, soil collapse induces a transient, as opposed to permanent, alteration in micropores, provided the material is subjected to a drying process (Yu et al. 2022). Moreover, the contraction of smaller macropores might have offset some micropore volume loss.

Ultimately, it is discernible that post-loading, the soil persistently exhibited two peaks in pore size, thereby sustaining the bimodal characteristic of the natural soil, a finding that aligns with the observations documented by Benatti and Miguel (2013) and Wang et al. (2018).

## Conclusions

The study conducted aims to analyze the collapsible behavior of clayey sand from Tuneiras do Oeste, Paraná, Brazil, utilizing one-dimensional compression tests following varied experimental procedures. The key conclusions drawn from the study are:

- **Moisture content and vertical stress:** The study evaluated the influence of moisture content (i.e., matric suction) and the vertical stress prior to soaking. Despite tests being conducted with the same initial moisture content, no monotonic relationship between collapse strains and pre-soaking vertical stress was observed. However, a monotonic relationship was derived between matric suction and collapse, indicating that as suction increases, so does the collapse

index. Hence, the collapse index is more sensitive to variations in suction than in vertical stress.

- **Influence of infiltration rate:** tests with a gradual increase in moisture showcased lower collapse index values, indicating the influence of the infiltration rate on such behavior. The conclusion is that as the infiltration rate increases, so does the collapse magnitude.
- **Pore size distribution:** MIP test results revealed a shift to the left in the frequency histograms of macropore size intervals, indicating a significant diameter reduction compared to natural soil samples without any loading. However, micropores did not exhibit significant changes. It was observed that the initial matric suction, directly related to collapse magnitude, did not significantly affect the final diameter peak values, but influenced the total pore volume. Therefore, a greater collapse magnitude results in a smaller total pore volume at the end of the process.
- **Collapse-predictive models application:** The collapse prediction model proposed by Pereira and Fredlund (2000) demonstrated satisfactory performance, with good adherence between predicted and experimental results for GIM tests, a determination coefficient greater than 0.98, and accurate definition of the three collapse phases for most tests. The two models developed in this study also showed qualitative satisfaction, with determination coefficients of 0.97 and 0.95 for the S tests and GIM tests, respectively. Considering the boundary conditions of the soil and tests, these models can be applied to predict collapsible behavior.
- **Conventional test efficacy:** The study concluded that good quality results can be achieved using a protocol with conventional tests, encouraging their use in scenarios where tests with control and imposition of suction are difficult to access.

**Acknowledgements** The authors thank the Coordination of Improvement of Higher Education Personnel (CAPES) for funding the research.

**Author contribution** Conceptualization: Renan Felipe Braga Zanin, Alana Dias de Oliveira, Amanda Maehara Kondo, and Raquel Souza Teixeira; methodology: Renan Felipe Braga Zanin, Amanda Maehara Kondo, and Avacir Casanova Andreello; formal analysis and investigation: Renan Felipe Braga Zanin, Amanda Maehara Kondo, Flávia Gonçalves Pissinati Pelaquim, Alana Dias de Oliveira, Sandro Lemos Machado, and Raquel Souza Teixeira; writing—original draft preparation: Renan Felipe Braga Zanin and Raquel Souza Teixeira; writing—review and editing: Renan Felipe Braga Zanin, Flávia Gonçalves Pissinati Pelaquim, Alana Dias de Oliveira, and Sandro Lemos Machado; supervision: Raquel Souza Teixeira. All the authors participated in the critical revision and approved the final version of the manuscript.

**Data availability** The data used to support the study is all included in the article.

## Declarations

**Conflict of interest** The authors declare no competing interests.

## References

- Al-Obaidi QA, Schanz T (2022) Deformation of unsaturated collapsible soils under suction control. *J Mech Behav Mater* 31:623–630. <https://doi.org/10.1515/jmbm-2022-0067>
- Alassal MA, Hassan AM, Elmamlouk HH (2023) Collapse potential prediction and characteristics of unsaturated sandy soils. *Geotech Geol Eng* 41:2759–2774. <https://doi.org/10.1007/s10706-023-02425-5>
- American Society for Testing and Materials (2017) D2487–17e1: Standard practice for classification of soils for engineering purposes (Unified Soil Classification System). ASTM International. West Conshohocken, PA, USA, p. 10. <https://doi.org/10.1520/D2487-17E01>
- American Society for Testing and Materials (2018) D4404: Standard test method for determination of pore volume and pore volume distribution of soil and rock by mercury intrusion porosimetry. ASTM International. West Conshohocken, PA, USA, p. 8. <https://doi.org/10.1520/D4404-18>
- American Society for Testing and Materials (2020) D2435/D2435M-11: Standard test methods for one-dimensional consolidation properties of soils using incremental loading. ASTM International. West Conshohocken, PA, USA, p. 14. [https://doi.org/10.1520/D2435\\_D2435M-11R20](https://doi.org/10.1520/D2435_D2435M-11R20)
- American Society for Testing and Materials (2021) D4546: Standard test methods for one-dimensional swell or collapse of soils. ASTM International. West Conshohocken, PA, USA, p. 10. <https://doi.org/10.1520/D4546-21>
- Associação Brasileira De Normas Técnicas (2016a) NBR 6458: Gravel grains retained on the 4.8 mm mesh sieve - determination of the bulk specific gravity, of the apparent specific gravity and of water absorption. ABNT. Rio de Janeiro, RJ, Brazil. (in Portuguese)
- Associação Brasileira De Normas Técnicas (2016b) NBR 6459: Soil - liquid limit determination. ABNT. Rio de Janeiro, RJ, Brazil. (in Portuguese)
- Associação Brasileira De Normas Técnicas (2016c) NBR 7180: Soil - Plasticity limit determination. ABNT. Rio de Janeiro, RJ, Brazil. (in Portuguese)
- Associação Brasileira De Normas Técnicas (2016d) NBR 7181: Soil - Grain size analysis. ABNT. Rio de Janeiro, RJ, Brazil. (in Portuguese)
- Baecher G, Christian J (2003) Reliability and statistics in geotechnical engineering. John Wiley&Sons Ltd., Chichester, England
- Basma AA, Tuncer ER (1992) Evaluation and control of collapsible soils. *J Geotech Eng* 118(10):1491–1504. [https://doi.org/10.1061/\(ASCE\)0733-9410\(1992\)118:10\(1491\)](https://doi.org/10.1061/(ASCE)0733-9410(1992)118:10(1491))
- Benatti JCB, Miguel MG, Rodrigues RA, Vilar OM (2011) Collapsibility study for tropical soil profile using oedometric tests with controlled suction. In: Proceedings of 5th International Conference on Unsaturated Soils. Barcelona, Spain, pp 193–198
- Benatti JCB, Miguel MG (2013) A proposal of structural models for colluvial and lateritic soil profile from southwestern Brazil on the basis of their collapsible behavior. *Eng Geol* 153:1–11. <https://doi.org/10.1016/j.enggeo.2012.11.003>
- Borges JJS, Torres MS, Veríssimo KJS, Freitas MLAA, Ferreira SEM (2016) Study of the flood effect on volume change, point resistance and modulus of elasticity of a collapsible soil in Pernambuco's semi-arid. *Matéria* 21(4):996–1011. <https://doi.org/10.1590/S1517-707620160004.0092>. (in Portuguese)
- Branco LP, Gomes AT, Cardoso AS, Pereira CS (2014) Natural variability of shear strength in a granite residual soil from Porto. *Geotech Geol Eng* 32:911–922. <https://doi.org/10.1007/s10706-014-9768-1>
- Das AP, Thyagaraj T (2016) Collapse behavior of compacted red soil. *Int J Geotech Eng* 12(1):20–27. <https://doi.org/10.1080/19386362.2016.1243506>
- Duncan J (2000) Factors of safety and reliability in geotechnical engineering. *J Geotech Geoenviron Eng* 126(4):307–316. [https://doi.org/10.1061/\(ASCE\)1090-0241\(2000\)126:4\(307\)](https://doi.org/10.1061/(ASCE)1090-0241(2000)126:4(307))
- Ercoli L, Zimbaro M, Nocilla N, Nocilla A, Ponzoni E (2015) Evaluation of cliff recession in the Valle dei Templi in Agrigento (Sicily). *Eng Geol* 192:129–138. <https://doi.org/10.1016/j.enggeo.2015.04.008>
- Ferreira SRM, Fucale SP (2014) Evaluation of the collapsibility of soils in the semiarid region of Pernambuco, Brazil. *J Civ Eng Archit* 8(10):1285–1292. <https://doi.org/10.17265/1934-7359/2014.10.010>
- Ferreira SEM (1995) Collapse and expansion of natural unsaturated soils due to wetting. Thesis, Federal University of Rio de Janeiro. Rio de Janeiro, RJ, Brazil. (in Portuguese)
- Fredlund DG, Xing A, Huang S (1994) Predicting the permeability function for unsaturated soils using the soil-water characteristic curve. *Can Geotech J* 31(4):533–546. <https://doi.org/10.1139/t94-062>
- Ge M, Pineda JA, Sheng D, Burton GJ, Li N (2019) Collapse behaviour of compacted loess: role of the stress level on soil microstructure. *Jpn Geotech Soc Spec Publ* 7(2):209–214. <https://doi.org/10.3208/jgsssp.v07.032>
- Giomi I, Francisca FM (2022) Numerical modeling of the oedometrical behavior of collapsible loess. *Geotech Geol Eng* 40:2501–2512. <https://doi.org/10.1007/s10706-021-02042-0>
- Gitirana GFN Jr, Fredlund DG (2004) Soil-water characteristic curve equation with independent properties. *J Geotech Geoenviron Eng* 130(2):209–212. [https://doi.org/10.1061/\(ASCE\)1090-0241\(2004\)130:2\(209\)](https://doi.org/10.1061/(ASCE)1090-0241(2004)130:2(209))
- Gutierrez NHM, Nóbrega MT, Vilar OM (2008) Influence of the microstructure in the collapse of a residual clayey tropical soil. *Bull Eng Geol Env* 68:107–116. <https://doi.org/10.1007/s10064-008-0180-z>
- Houston SL, Houston WN, Zapata CE, Lawrence C (2001) Geotechnical engineering practice for collapsible soils. *Geotech Geol Eng* 19:333–355. <https://doi.org/10.1023/A:1013178226615>
- Jennings JE, Knight K (1957) The additional settlement of foundation due to a collapse of structure of sandy subsoils on wetting. In: Proceedings of 4th International Conference on Soil Mechanics and Foundation Engineering. London, UK, pp 316–319
- Jennings JE, Knight K (1975) A guide to construction on or with materials exhibiting additional settlement due to a collapse of grain structure. In: Proceedings of 4th Regional Conference for Africa on Soil Mechanics and Foundation Engineering. Durban, South Africa, pp 99–105
- Jiang M, Zhang F, Hu H, Cui Y, Peng J (2014) Structural characterization of natural loess and remolded loess under triaxial tests. *Eng Geol* 181:249–260. <https://doi.org/10.1016/j.enggeo.2014.07.021>
- Li P, Xie W, Pak RYS, Vanapalli SK (2019) Microstructural evolution of loess soils from the Loess Plateau of China. *Catena* 173:276–288. <https://doi.org/10.1016/j.catena.2018.10.006>
- Li P, Vanapalli SK (2018) Simple method for prediction of the soil collapse behavior due to wetting. *Int J Geomech* 18(11):06018026(1–5). [https://doi.org/10.1061/\(ASCE\)GM.1943-5622.0001285](https://doi.org/10.1061/(ASCE)GM.1943-5622.0001285)
- Li ZS, Derfouf FEM, Benchouk A, Abou-Bekr N, Taibi S, Fleureau JM (2018) Volume change behavior of two compacted clayey soils under hydraulic and mechanical loadings. *J Geotech Geoenviron Eng* 144(4):04018013(1–14). [https://doi.org/10.1061/\(ASCE\)GT.1943-5606.0001851](https://doi.org/10.1061/(ASCE)GT.1943-5606.0001851)
- Machado SL, Zuquette LV (2004) Mass transport and retention mechanism in unsaturated soils. In: Proceedings of 5th Brazilian Symposium on Unsaturated Soils. São Carlos, SP, Brazil, pp 545–572. (in Portuguese)

- Öberg AL, Sällfors G (1997) Determination of shear strength parameter of unsaturated silts and sands based on the water retention curve. *Geotech Test J* 20(1):40–48. <https://doi.org/10.1520/GTJ11419J>
- Oliveira AD, Pelaquim FGP, Zanin RFB, Melo TR, Tavares Filho J, Andreello AC, Teixeira RS (2022) The structure of tropical lateritic soils as an impacting factor in the shape of soil-water characteristic curves. *Soils Rocks* 45(2):e2022070521. <https://doi.org/10.28927/SR.2022.070521>
- Pereira JHF, Fredlund DG (2000) Volume change behavior of collapsible compacted gneiss soil. *J Geotech Geoenviron Eng* 126(10):907–916. [https://doi.org/10.1061/\(ASCE\)1090-0241\(2000\)126:10\(907\)](https://doi.org/10.1061/(ASCE)1090-0241(2000)126:10(907))
- Pereira JHF, Fredlund DG, Cardão Neto MP, Gitirana GF Jr (2005) Hydraulic behavior of collapsible compacted gneiss soil. *J Geotech Geoenviron Eng* 131(10):1264–1273. [https://doi.org/10.1061/\(ASCE\)1090-0241\(2005\)131:10\(1264\)](https://doi.org/10.1061/(ASCE)1090-0241(2005)131:10(1264))
- Phanikumar BR, Raghav R, Bhargav K (2016) Collapse behaviour of a lateritic soil. *Geomech Geoeng Int J* 11(2):119–124. <https://doi.org/10.1080/17486025.2015.1042925>
- Phoon K-K, Kulhawy FH (1999) Characterization of geotechnical variability. *Can Geotech J* 36(4):612–624. <https://doi.org/10.1139/t99-03>
- Rao SM, Revanasiddappa K (2002) Collapse behaviour of a residual soil. *Géotechnique* 52(4):259–268. <https://doi.org/10.1680/geot.2002.52.4.259>
- Romero E, Della Vecchia G, Jommi C (2011) An insight into the water retention properties of compacted clayey soils. *Géotechnique* 61(4):313–328. <https://doi.org/10.1680/geot.2011.61.4.313>
- Shao X, Zhang H, Tan Y (2018) Collapse behavior and microstructural alteration of remolded loess under graded wetting tests. *Eng Geol* 233:11–22. <https://doi.org/10.1016/j.enggeo.2017.11.025>
- Silva WP, Silva CMDPS (2022) LAB Fit Curve Fitting Software (Nonlinear Regression and Treatment of Data Program) Version 7.2.50c. LAB Fit. <http://www.labfit.net/index.htm>. Accessed 28 Aug 2023
- Silva Filho FC, Moura AS, Futai MM (2010) A solution for collapsible soil foundations on the UFC Campus in Cariri. In: *Proceedings of 15th Brazilian Congress of Soil Mechanics and Geotechnical Engineering*. Gramado, RS, Brazil. (in Portuguese)
- Van Genuchten MT (1980) A closed-form equation for predicting the hydraulic conductivity of unsaturated soils. *Soil Sci Soc Am J* 44(5):892–898. <https://doi.org/10.2136/sssaj1980.03615995004400050002x>
- Vilar OM, Davies GI (2001) Collapse behavior analysis of a clayey sand using different testing procedures. In: *Proceedings of 4th Brazilian Symposium on Unsaturated Soils*. Porto Alegre, RS, Brazil, pp 354–376. (in Portuguese)
- Vilar OM, Rodrigues RA (2011) Collapse behavior of soil in a Brazilian region affected by a rising water table. *Can Geotech J* 48(2):226–233. <https://doi.org/10.1139/T10-065>
- Wang JD, Li P, Ma Y, Vanapalli SK (2018) Evolution of pore-size distribution of intact loess and remolded loess due to consolidation. *J Soils Sediments* 19:1226–1238. <https://doi.org/10.1007/s11368-018-2136-7>
- Wang JD, Li P, Ma Y, Vanapalli SK (2020) Change in pore-size distribution of collapsible loess due to loading and inundating. *Acta Geotech* 15:1081–1094. <https://doi.org/10.1007/s11440-019-00815-9>
- Yu CY, Chow JK, Wang YH (2016) Pore-size changes and responses of kaolinite with different structures subject to consolidation and shearing. *Eng Geol* 202(4):122–131. <https://doi.org/10.1016/j.enggeo.2016.01.007>
- Yu B, Fan W, Dijkstra TA, Wei YN, Deng LS (2021) Heterogeneous evolution of pore structure during loess collapse: insights from X-ray micro-computed tomography. *CATENA* 201:105206. <https://doi.org/10.1016/j.catena.2021.105206>
- Yu B, Fan W, Dijkstra TA, Wei YN, Deng LS (2022) Pore structure evolution due to loess collapse: a comparative study using MIP and X-ray micro-CT. *Geoderma* 424:115955. <https://doi.org/10.1016/j.geoderma.2022.115955>
- Zamani M, Badv K (2019) Assessment of the geotechnical behavior of collapsible soils: a case study of the Mohammad-Abad Railway Station soil in Semnan. *Geotech Geol Eng* 37:2847–2860. <https://doi.org/10.1007/s10706-018-00800-1>
- Zeng G, Meng X (2006) Experimental study on the relationship between moisture content and deformation of collapsible loess. In: *GeoShanghai International Conference – Advances in Unsaturated Soil, Seepage, and Environmental Geotechnics*. Shanghai, China, pp 136–142. [https://doi.org/10.1061/40860\(192\)13](https://doi.org/10.1061/40860(192)13)
- Zorlu K, Kasapoglu KE (2009) Determination of geomechanical properties and collapse potential of a caliche by in situ and laboratory tests. *Environ Geol* 56:1449–1459. <https://doi.org/10.1007/s00254-008-1239-7>

Springer Nature or its licensor (e.g. a society or other partner) holds exclusive rights to this article under a publishing agreement with the author(s) or other rightsholder(s); author self-archiving of the accepted manuscript version of this article is solely governed by the terms of such publishing agreement and applicable law.